Characterization of clouds from PFS observations and MARCI images in the Tharsis region during the dusty season.

P. Wolkenberg, *Istituto Nazionale di Astrofisica, Istituto di Astrofisica e Planetologia Spaziali (INAF-IAPS), Rome, Italy (paulina.wolkenberg@inaf.it),* **J. Hernandez-Bernal,** *LMD/IPSL, Sorbonne Université, ENS Paris, Université PSL, CNRS, École polytechnique, Institut polytechnique de Paris, Paris, France*, **M. Giuranna**, *Istituto Nazionale di Astrofisica, Istituto di Astrofisica e Planetologia Spaziali (INAF-IAPS), Rome, Italy*

Introduction:

We study the seasonal variability of aerosols during the northern fall and winter seasons in the Tharsis region of Mars in MYs 28, 31, 34 and 35. We used PFS observations [1] quasi-simultaneously with images taken by the MARCI camera [2]. The clouds were observed in the afternoon. Using MARCI images, thermal fields retrieved from PFS observations [3, 4, 5] and using water vapor mixing ratios taken from the MCD model [6, 7], we will investigate the altitudes of the hygropause. This will help us determine the possible heights at which clouds occur and study their origin. We will investigate the atmosphere over each volcano separately.

Clouds:

After analyzing MARCI images, we found that clouds occur in three preferred L_s ranges (180° – 210°, 240° – 270° and 330° – 360°) except in years with the GDSs (global dust storms). We define the dusty season as the L_s ranging from 180° to 360°. We found that clouds mostly occur in the afternoon, around 14-16 LT, during the first period of L_s. They likely persist after formation during the aphelion season. The clouds persist until around L_s = 200° - 210° in all years considered. However, clouds were observed over Arsia before the GDS in MY34 (L_s = 180° – 190°).

The next period of cloud activity occurs at L_s between 240° and 270° (Table 1). In this range of L_s, clouds occurred around all volcanoes in MY 28 but their activity ended earlier because the GDS started around L_s = 265°. The clouds over the volcanoes disappeared at L_s = 280° in MY 31. In MY34, cloud formation around all volcanoes began later at L_s = 270° due to the GDS that year. The clouds are very thin. In MY 35, cloud activity is limited to Ascraeus and Pavonis only (Table 1). In this L_s range, clouds form as filaments extending south of Ascraeus.

Interestingly, the clouds were also observed in the last range of L_s from 330° to 360°, but between 13 and 14 LT, which is one hour earlier than in the first range of L_s. This L_s range corresponds with the period just after dust event type 'C' occurs. In MY28, clouds were observed over Ascraeus, Arsia, and Pavonis in one image. No data are available for Olympus in this year. In MY31, MARCI images show clouds over all volcanoes except Pavonis. The clouds are mostly visible over the eastern flank of Olympus. In MY34, clouds are evident only over Pavonis and Arsia; images of the other volcanoes are clear and cloudless. In MY35, clouds are only present over Pavonis and Ascraeus.

Table 1. Seasonal variability of clouds from MARCI.

L_s range and MY	Pavonis	Ascraeus	Olympus	Arsia
L_s = 240 – 270 MY28	X	X (1 image)	X (1 image) (L_s = 246)	X (until L_s = 265)
L_s = 240 – 270 MY31	X (L_s = 234 – 268)	X (L_s = 260-275)	X (L_s = 270 – 280)	X (until L_s =270)
L_s = 240 – 270 MY34	X (L_s = 280 - 313)	X (L_s = 290 – 310)	X (L_s = 290)	X (L_s = 240 – 247)
L_s = 240 – 270 MY35	X (L_s = 260 – 300)	X (L_s = 270 – 310)	-	-
L_s = 330 – 360 MY28	X (1 image)	X	No data	X (L_s = 323 – 353)
L_s = 330 – 360 MY31	-	X (L_s = 343 – 360)	X (L_s = 332 - 360)	X (L_s = 321 – 350)
L_s = 330 – 360 MY34	X (L_s = 340 – 350)	-	-	X (L_s = 290 - 315) (Ls = 332 – 355)
L_s = 330 – 360 MY35	X	X (L_s = 350 – 360)	-	-

Olympus.

We can discern three intervals of L_s when clouds form over Olympus during the dusty season. During all three intervals, clouds are observed by both PFS and MARCI. In MY28, we observed clouds almost simultaneously during the same days using MARCI images for three PFS orbits in the first L_s range. Figure 1 shows PFS observations (orbit 3996), which were taken approximately three hours after the

MARCI image. We observe some local increases in water ice opacity up to 0.4 by PFS. As seen in the right panel of Fig.1, the PFS footprint is very small and crosses the west flank of Olympus, whereas the water ice clouds are mostly found over the east flank, caldera, and valley of the volcano. The clouds covered a vast area east, north and south of Olympus (Fig. 1).

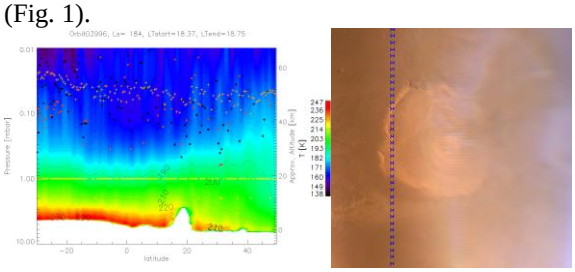

Figure 1. Left panel presents thermal fields of orbit 3996 with water ice opacities as black dots (L_s = 184.5, LT = 18.5, UTC = 15/02/2007, 14:43:00). Red points present dust opacities. Yellow circles present chi-squares less than 1.5 and corresponding MAPE as orange pluses. Right panel presents the MARCI image (L_s = 184.4, LT = 15.7, UTC = 15/02/2007, 11:49:22) with the PFS footprint for orbit 3996.

In MY 31, we observed clouds within the first L_s range using MARCI images. We found only one PFS orbit (11193), which was measured two days before the first MARCI image. Two images were taken two and five days after the PFS orbit.

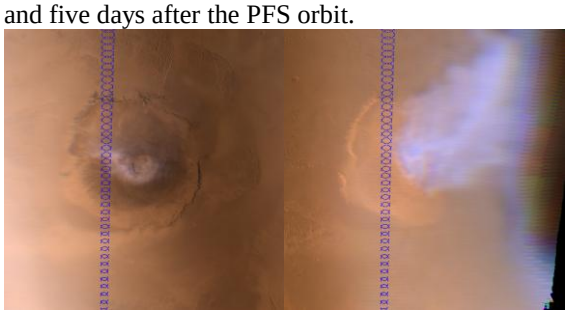

Figure 2. Left panel presents the MARCI image taken at L_s = 191.6, LT = 14.7, UTC = 19/10/2012, 22:14:04. Right panel presents the MARCI image taken at L_s = 192.8, LT = 15.8, UTC = 22/10/2012, 00:43:05 with the PFS footprint for orbit 11193.

The left MARCI image, taken two days after the PFS orbit shown in Fig. 2, shows very thin clouds over the caldera and the western flank of Olympus. The right MARCI image, taken 5 days later at LT around 16, shows a large and thick cloud over the eastern and northern flanks of the volcano and the region northeast of it. The PFS observes 0.2 of water ice opacities over the caldera and cold temperatures close to the surface of the volcano's top. According to the MARCI images, we observe cloud growth within 2 hours, from 14 LT to 16 LT. More evident clouds usually occur after 15 LT northeast of Olympus.

In MY35, MARCI images also show clouds in the first L_s range. These clouds mostly occur over the northeastern flank and valley, as was observed in previous years at 15 LT or later. In some cases, the clouds are thin over the caldera. In the next L_s interval, clouds appear over the volcano in MY 28, MY31 and MY34.

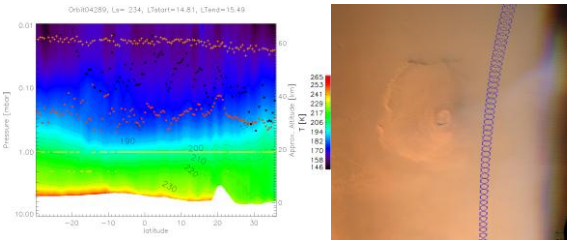

Figure 3. Left panel presents thermal fields of orbit 4289 with water ice opacities as black dots (L_s = 234.1, LT = 14.9, UTC = 08/05/2007, 16:08:00). Right panel presents the MARCI image (L_s = 234.1, LT = 15.4, UTC = 08/05/2007, 16:37:38) with the PFS footprint for orbit 4289.

Fig. 3 shows an example of clouds from slightly earlier period. Quasi-simultaneous observations by MARCI and PFS were taken at L_s = 234.1 and LT around 15 in MY 28 (Fig. 3). The PFS measurement occurred 30 minutes before the MARCI image. Water ice opacities vary from 0.2 to 0.06 near and over the east flank in the PFS orbit 4289. The MARCI image shows clouds and dust over the east flank and eastward of this region. The clouds do not exhibit oscillations in water ice opacity as observed by the PFS, possibly due to mountain gravity waves. Perhaps the rapid cloud formation is why we do not observe the large water ice opacities in the PFS observations, which were taken early in the afternoon.

In MY 31, clouds form after L_s = 270° and persist until L_s = 280°. They form around the caldera and the east flank of the volcano. In MY 34, clouds are evident over the east flank around L_s = 289°, possibly representing gravity waves in the MARCI images. In MY35, no clouds were observed during this period. We also observed clouds in the MARCI images in the afternoon after L_s = 330° in MY31. However, the clouds appear earlier in LT (13-14) than in the initial L_s range. They mostly occur northeast of the caldera. No data was delivered in MY 28 during this period. In MY 34 and 35, no clouds were observed over this volcano during this time. Clouds are mostly observed over the caldera, the east flank, and the region northeast of the volcano.

Pavonis.

MARCI images in MY 28 also observed clouds around Pavonis in the first L_s range. The corresponding PFS orbit, 4091, was measured around 15 hours after the MARCI image. A large amount of water ice opacity is observed around 1 on the south side of Pavonis. The results from both instruments are con-

sistent.
In MY 31, clouds appear during the initial L_s interval. They are observed as a filament connected with Arsia and around the caldera of Pavonis. In MY34, the GDS prevents visibility of clouds during the first L_s range. In MY35, the MARCI images show that the clouds are distributed around and cover the volcano in the first L_s range. No coincident PFS observations in time are found for this period.
In the second L_s range, we observe clouds around Pavonis, as well as a filament connected to Arsia, in MY 28. In MY 31, the clouds form slightly earlier than in the second L_s range, at L_s = 234° (Table 1). In MY34, the season starts later and begins at L_s = 280°. Six cases of different types of clouds occur: three are west and south elongated. Perihelion cloud trails (PCTs) [8] are found around Pavonis in two cases, and in one case, they are connected with Arsia as a filament. This period has many clouds, mostly connected with Arsia and west-elongated. Compared to perihelion cloud trails, clouds around Pavonis occur sporadically. However, their morphology is similar to that of the PCTs. The second L_s range in MY35 starts from L_s = 258° to L_s = 300°.

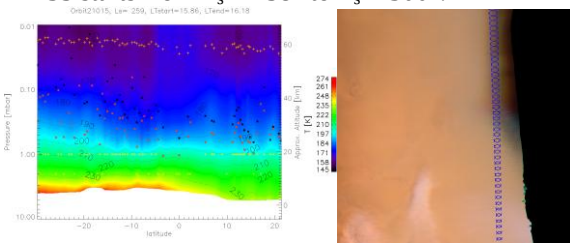

Figure 4. Right panel presents the MARCI image taken at L_s = 259.3, LT = 15.5, UTC = 16/08/2020, 09:18:59 with the PFS footprint for orbit 21015. Left panel presents thermal fields retrieved from the PFS observation (orbit 21015) at L_s = 259.3, LT = 15.9, UTC = 16/08/2020, 09:44:00.

An example of a mixture of dust and water ice clouds is shown in Fig. 4 within the second L_s range. PFS observations (21015) were taken approximately 30 minutes after the MARCI image on the same day (Fig. 4). The PFS footprint crosses a region that is blurred in the image. However, the MARCI image shows clouds between Pavonis and Arsia that are not included in the PFS footprint. Nevertheless, the PFS water ice and dust opacities are high around Pavonis.
In the third L_s range, after dust events of type C, filament-like clouds are observed over the west side of Pavonis, connected with Arsia, at LT 14.4 in MY 28 and MY 35. Some clouds are also observed around the volcano, although the images are of poor quality in MY 31. In MY 34, clouds occur south of the volcano. In MY35, some clouds are distributed around Pavonis, with a few occurring over the east side of Pavonis. Clouds often cover Pavonis volcano, forming a southwestern filament connected with Arsia volcano. Clouds are also found over the east side of Pavonis in the third L_s range.

Ascraeus.
In MY28, clouds are mostly visible on the east side of Ascraeus, and, in one case, over the west side of the volcano within the first L_s range, as seen in MARCI images. They are mostly very thin over the Ascraeus caldera.

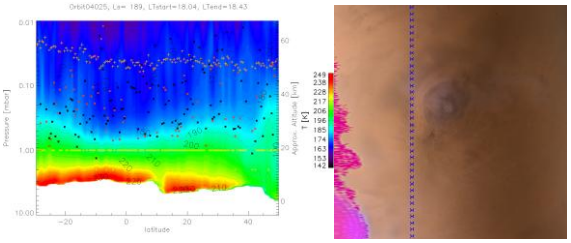

Figure 5. Right panel presents the MARCI image taken at L_s = 189, LT = 14.9, UTC = 23/02/2007, 14:18:16 with the PFS footprint for orbit 4025. Left panel presents thermal fields retrieved from the PFS observation (orbit 4025) at L_s = 189.1, LT = 18.2, UTC = 23/02/2007, 17:39:43.

Clouds form early over the west side of Ascraeus in time at LT = 14.9, and PFS also observes them 3 hours later in Fig. 5 in MY28. In MY31, clouds are mostly observed over the east side of volcano in the first L_s range. Some clouds are also visible over the caldera. There are two cases of clouds over the west side of the volcano. The PFS orbit is measured six hours later, at LT = 21, than the MARCI image, which shows clouds over the east side of Ascraeus. However, the PFS footprint does not cover the region with clouds. Thus, the PFS observes no clouds. In MY 34, a GDS interrupted the cloud occurrences in the first L_s range. In MY35, clouds were mostly observed over the east side of Ascraeus within the first L_s range. During this period, three cases of clouds over the western side of Ascraeus were observed. Additionally, four cases of clouds over the caldera and as a south filament extending to Pavonis were observed. In the second L_s interval, a south filament of clouds is observed at L_s = 259° in MY 28. However, there is a gap in the images between L_s = 263° and L_s = 286°, which is when the GDS started. In MY31, clouds appear as a filament moving southward within the second L_s range (Fig. 6). The occurrence of clouds alternates between a southern filament and the caldera, shifting by 20° of L_s over time with respect to the second L_s range in MY34, probably due to the GDS, and in MY35. By the end of this period, clouds are visible on the east side of the volcano at L_s = 313°. In the third L_s range, clouds are again observed over the caldera and the east-north side of MY 28 as with Olympus. Clouds are very thin, and are absent after 5 hours in the PFS observation. In the third L_s range, clouds are mostly visible over the caldera in MY 31. No clouds occurred during the third period after the ‘C’ type of dust event in

MY 34. During the third period, clouds mostly cover the eastern side of Ascreaus at the end of MY 35. One case of clouds as a southern filament and one case of clouds to the west are observed during this period. Clouds are mostly observed on the eastern side and flank of Ascraeus. Sporadically, clouds occur as a filament over the southwest side. The clouds are very thin over the caldera.

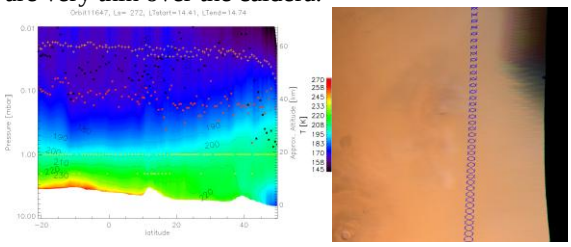

Figure 6. Right panel presents the MARCI image taken at L_s = 271.9°, LT = 14.8, UTC = 26/02/2013, 08:30:45 with the PFS footprint for orbit 11647. Left panel presents thermal fields retrieved from the PFS observation (orbit 11647) at L_s = 271.9°, LT = 14.6, UTC = 26/02/2013, 08:13:35.

Arsia.

In MY28, clouds began to form at L_s = 182°. They covered the southeastern side of the volcano and the southwestern region. They mostly occurred after 15:00 LT to 16:00 LT in groups with one or two days of pause until L_s = 237°. In MY31, clouds again, started forming at L_s = 192°. We do not know if clouds occurred earlier because we did not analyze the data. These clouds were observed with a pause of two or so until L_s = 209°. They cover the southernwestern region of Arsia, or alternatively the southern and northeastern regions of Arsia. Two cases of PCT clouds were observed, but it is too early in L_s for more cases to occur. From L_s = 209° to L_s = 229°, a regional dust storm occurs over the southern region of Arsia in MY 31. In MY34, clouds were observed before the onset of GDS within the initial L_s range. In MY 35, clouds appear later in this L_s range, at L_s = 206°. They continue to form until L_s = 229°, mostly over the southern western region of Arsia. Three cases of textured dust are observed at L_s = 206°, 209° and 212° during this period.

In the second L_s range, clouds appear before the GDS begins in MY 28. During this period, two cases of PCT clouds appear alongside the northern east filament. Then, clouds are mostly observed over the southern western region of Arsia. More cases of PCT clouds and the northern east filament are observed during this time until L_s = 260° in MY 31. Then, there is a pause of 3° in L_s. After this pause, clouds are mostly observed over the southern western region of Arsia until L_s = 270°. From L_s = 240°, clouds are observed for a short period until L_s = 246° over the southern or southwestern side of Arsia in MY 34. In the second L_s range, cloud occurrence starts at L_s = 294°. Clouds are observed until L_s = 315°, with pauses of about 1 day. During this period, textured dust was unexpectedly observed around Arsia. No clouds and dust were observed in MY 35 during this season.

In the third L_s interval, clouds are mostly observed over the southern and southwestern region from Arsia in MY 28. One case of eastern clouds is observed. Cloud formation starts earlier in this period, beginning at LT 13. Clouds start forming earlier than in the third L_s range in MY 31. However, pauses in cloud formation are evident again. Clouds are observed over the southwestern side of Arsia.

Eventually, dust becomes visible in the MARCI images at L_s = 327° on the eastern side of Arsia during a 'C' type event. After this type 'C' dust event, clouds were again observed over the southern western region in MY 34. An example of this is shown in the MARCI image at L_s = 355°. During this season, no clouds were visible over and around Arsia in MARCI images in MY 35. Clouds are mostly observed over the western southern region from Arsia. During the second L_s range, PCT clouds and northeastern filaments connected with Pavonis are observed. The formation of clouds during the third L_s range occurs between 13 and 14 LT, which is one hour earlier than the first L_s range.

Summary and conclusions:

Clouds are mostly observed over the caldera and the east flank, as well as the region northeast of Olympus for all considered MYs and three L_s ranges. Clouds cover Pavonis and often occur as southwest filaments connected with Arsia. In the third L_s range, clouds are also found on the east side of Pavonis. Clouds are mostly observed over the east flank and side of Ascraeus. Sporadically, clouds occur over the southwest side as filaments connected with Pavonis. Clouds are very thin over the caldera. Most clouds are observed over western southern region from Arsia. In the second L_s range, PCT clouds and northeastern filaments connected with Pavonis are observed. The formation of clouds during the third L_s range occurs between 13 and 14 LT, one hour earlier than the first L_s range.

Bibliography:

[1] V. Formisano, et al. (2005), Volume 53, Issue 10, 963-974. [2] Bell, J. F.III, et al. (2009), *J. Geophys. Res.*, 114, E08S92. [3] Grassi D., et al. (2005), Planetary and Space Science, Volume 53, Issue 10, 2005, 1017-1034. [4] Wolkenberg, P., et al., (2018), Icarus, 310, 32–47. [5] M. Giuranna, et al. (2021), Icarus, 353, 113406. [6] Forget, F., et al. (1999), *J. Geophys. Res.*, 104 (E10), 24155–24175. [7] Millour et al. (2018), THE MARS CLIMATE DATABASE (VERSION 5.3), Scientific Workshop: "From Mars Express to ExoMars" 27–28 February 2018, ESAC Madrid, Spain. [8] Clancy T. et al. (2021), Icarus, 362, 114411.